Presented at Symposium on Plasma Heating & Injection, Sept 21-Oct 4, 1972, Varenna, Italy

CONF-720961--11

PLASMA HEATING BY ADIABATIC COMPRESSION

R. A. Ellis, Jr.
Plasma Physics Laboratory, Princeton University,
Princeton, New Jersey 08540

MASTER

ABSTRACT

These two lectures will cover the following three topics: (i) The application of adiabatic compression to toroidal devices will be reviewed. The special case of adiabatic compression in tokamaks will be considered in more detail, including a discussion of the equilibrium, scaling laws, and heating effects. (ii) The ATC (Adiabatic Toroidal Compressor) device which was completed in May 1972, will be described in detail. Compression of a tokamak plasma across a static toroidal field is studied in this device. The device is designed to produce a pre-compression plasma with a major radius of 17 cm, toroidal field of 20 kG, and current of 90 kA. The compression leads to a plasma with major radius of 38 cm and minor radius of 10 cm. Scaling laws imply a density increase of a factor 6, temperature increase of a factor 3, and current increase of a factor 2.4. An additional feature of ATC is that it is a large tokamak which operates without a copper shell. (iii) Data which show that the expected MHD behavior is largely observed will be presented and discussed.

I. INTRODUCTION

The fact that simple Ohmic heating is insufficient to heat tokamaks to ignition temperatures serves to keep attention directed to alternative methods of heating tokamaks.

The subject of these lectures is the application of adiabatic compression to the heating of tokamak plasmas. Of the several methods of application of compressional heating in tokamaks, we will be mainly concerned with the compression associated with decreasing the major radius in a static toroidal field.

Such a method was proposed by Artsimovich[1] in which the change in major radius was considered to be carried out on a time scale short compared with the like particle collision times. The method emphasized here[2] is a collisional adiabatic compression, by which we mean that the time of compression is slow compared with ion-ion and electron-electron collision times, but fast compared with the energy loss time.

The experimental investigation of adiabatic compression at the Plasma Physics Laboratory has centered about the ATC (Adiabatic Toroidal Compressor) device. The particular choice of design of ATC also permits investigation of the properties of a tokamak which does not have a conducting shell.

Section II contains a discussion of the plasma equilibrium, and scaling laws related to adiabatic compression; Sec. III consists of a description of the ATC device and Sec. IV contains a discussion of some data obtained on ATC which show that the MHD behavior of the plasma is in general agreement with the theory.

II. EQUILIBRIUM AND SCALING LAWS

The equilibrium problem of the plasma undergoing a "slow" adiabatic compression is, for practical purposes, the same as that for a plasma with fixed major and minor radii because, if the compression is slow enough, it can be treated as quasi-static and we consider the plasma to go through a succession of equilibria as the compression proceeds.

The equilibrium of toroidal currents in toroidal magnetic fields has been reviewed recently.[3] The case in which the equilibrium is produced by means of a conducting shell is perhaps most familiar (conventional tokamak), but it has been recognized from the beginning that it is possible to provide the necessary equilibrium vertical field with a system of poloidal field coils.[3,4] For major radius compression a detailed examination of the equilibrium has been carried out[5] which shows that the theory of Shafranov is sufficient for a simple description of the process and that there exists a suitable field configuration.

The assumption that the process is quasi-static means that the equilibrium vertical field satisfies the relations in Eqs. (1) and (2) at each stage of the compression and that effects of acceleration are neglected.

$$B_v = \frac{I_p}{cR}\left(\ln\frac{8R}{a} + \beta_p + \frac{\ell_i}{2} - \frac{3}{2}\right) \qquad (1)$$

where B_v is the equilibrium vertical field, I_p is the plasma current, R and a are the major and minor radii,

$$\beta_p = 4\pi(\langle p_\perp\rangle + \langle p_\parallel\rangle)/B_T(a)^2$$

is the poloidal Beta, and ℓ_i is the internal inductance per unit length of the plasma current distribution.

If we write $n = -(R/B_v)(\partial B_v/\partial R)$, then we can give the condition for vertical and radial stability as

$$0 < n < 3/2 \qquad (2)$$

One of our primary tasks is to provide the proper vertical field, B_v during the compression and we will note for future reference that in major radius compression the variation of B_v provides the main compressive motion.

The experimental study of the MHD stability of tokamaks without conducting liner is just beginning, and we must use theory[6] as a guide. (We will present below some data from ATC on this question.)

The calculations suggest that the conducting liner has a strong stabilizing effect only on the high-m modes of the kinks and a relatively small effect on the m = 1,2 modes. Thus, the observed stability in many conventional tokamak experiments is probably due to shear or minimum-B stabilization. We have adopted the view that (subject to experimental verification) at sufficiently high q ($q = 5a^2B_T/RI_p$), say, q > 3, the plasma will be stable in the absence of a conducting liner.

The scaling laws for magnetic compression are worked out in Ref. 2. They are derived for infinite conductivity, which implies the following two relations:

$$a^2 B_T = \text{const} \qquad (3)$$

$$\ell \text{ or } q = \text{const} \qquad (4)$$

DISTRIBUTION OF THIS DOCUMENT UNLIMITED

where a is the minor radius of the plasma column, B_T is the toroidal field; and $\iota = 2\pi/q$ is the rotational transform. We also assume that the compression is collisional which means

$$T\, n^{-2/3} = \text{const} \qquad (5)$$

where T is the ion or electron temperature, n is the density, and we have taken $\gamma = 5/3$.

From Eqs. (3) - (5), we can obtain the following scaling laws shown in Table I for three modes of compression.

Compression in minor radius at constant major radius can be carried out by raising the toroidal field. This also requires an increase in B_v to maintain the equilibrium (Eq. (1)). This type of compression requires a large increase in the total magnetic energy and results in a larger aspect ratio, R/a. This is a technically feasible method of compressional heating and there are experiments planned to test its effectiveness. Note, however, that the plasma energy scales with magnetic energy, W_m as $W_p \sim W_m^{1/3}$, which means that a large increase in W_m leads to a small increase in W_p.

It is possible to carry out compression in both major and minor radii in the two modes illustrated in Fig. 1. In the type of compression labeled A in Table I, the aspect ratio is maintained during the compression. The toroidal field increases, but compared with constant-R compression, the plasma energy scales more favorably with magnetic energy, $W_p \sim W_m$. Nevertheless, the pulsed magnetic energy required to heat the plasma is large.

The type-B compression in Table I and Fig. 1, which is utilized in ATC, has the feature that the compression is carried out with constant (B_T), which means that the total magnetic energy remains almost constant. As the major radius is reduced the plasma is forced into a region of larger toroidal field, which implies a reduction of minor radius (Eq. (2)), $a \sim R^{1/2}$. The pulsed magnetic field is the B_v which has energy comparable to the plasma energy, W_p, which is much smaller than W_m. A further property of this mode of compression is that the aspect ratio improves, and that β_T increases more than β_p. A disadvantage of type-B compression is that the initial plasma may have a relatively unfavorable aspect ratio.

Note that the adiabatic compression technique is not strictly speaking a heating method, since no irreversible process is involved. The idea is rather to make better use of Ohmic dissipation by carrying out the Ohmic heating phase at large major radius and then transforming the plasma parameters to small major radius. Since the initial state in this transformation is necessarily a low-field low-current state, it is not obvious that any plasma heating advantage is to be gained by the compression, as compared with a simple Ohmic-heating phase that makes use of the whole available volume. Indeed, one can easily verify by numerical examples that for present-day tokamak plasma parameters, or in any experiments with modest radial compression factors, the final plasma temperature cannot be improved appreciably by the compression technique. The advantages of the radial compression transformation are found to be quite specialized. For example, as is shown in Ref. 2, a main virtue of the transformation is that in future experiments with large compression factors it will permit the barrier of radiation cooling to be overcome, allowing the Ohmic dissipation process to carry the tokamak plasma to thermonuclear ignition. As is well known, this could not be done under plausible confinement assumptions by a simple Ohmic heating phase alone.

The original radial magnetic pumping scheme suggested in Ref. 1 is of quite a different character in several respects. It provides a real heating effect: the compression cycle is carried out in roughly an ion-ion collision-time, so that a temperature anisotropy results, the collisional relaxation of which provides an element of irreversibility. The temperature can thus be raised continuously. A second important difference relative to the scheme of Ref. 2, however, is difficulty of technical implementation.

The high frequencies required by Ref. 1 create severe problems of vertical field penetration through the tokamak vacuum vessel; since the heating per cycle is typically quite small, the plasma must also be driven through a large number of cycles. Accordingly this scheme has not yet been implemented experimentally, and could not be implented, for example, on the present ATC device. We note, finally that the transformation of parameters by compression should be useful in conjunction with non-Ohmic initial heating methods: for example, neutral injection or ion cyclotron heating.

III. THE ATC DEVICE

The ATC device was built to test the type-B compression. The design called for production of a pre-compression plasma with T-3 (circa mid 1970) parameters, i.e., $n_e = 2 - 3 \times 10^{13}$, plasma current ≈ 70 kA, major and minor radii of R = 90 cm and a = 17 cm, respectively, electron and ion temperature of 1Kev and 500 eV, respectively, and toroidal field of 20 kG at R = 90 cm. The design called for a compressed plasma major radius of 38 cm. ($C \approx 2.37$) for which Table I gives $n_o/n_1 = 5.6$, $T_1/T_o = 3$, $I_{pl}/I_{po} = 2.4$, $B_{T1}/B_{To} = 2.4$, and $a_o/a_1 = 1.5$.

As noted above, type-B compression requires a static toroidal field and a variable vertical compression field. The requirement of large change in major radius during compression necessitates the use of an air-core transformer rather than iron because the toroidal field coils extend nearly to the axis of the torus. The use of a conducting liner was never considered and the vertical equilibrium field coils are programmed to produce the compression.

A cutaway view of the ATC is shown in Fig. 2 and a schematic view of a cross section is shown in Fig. 3. Table II shows some of the characteristics of the toroidal field magnet. An interesting feature of the toroidal field coils is that they are designed to be self supporting without the use of coil cases. This goal was achieved with a small safety factor by fabrication from copper with high tensile yield strength. The time between discharges is about 3 minutes at maximum field and is determined by the cooling of the toroidal field coils.

The vacuum vessel was developed to meet the conditions that the vertical field and Ohmic heating transformer coils should be outside the vacuum and that it should have a high electrical resistance. The first of these requirements imposes the configuration shown in Figs. 2 and 3 and, for the second, an insulator would be preferable, but extremely difficult to manufacture. The choice

of a 0.75 mm stainless steel bellows was made because it could meet the requirement of relatively low conductivity indeed, the bellows construction both improves the strength and increases the electrical resistance) and relatively simple, if tedious, to produce. It consists of about 800 lamina welded to form a bellows with six pumping, and diagnostic ports. After final assembly, the vessel is sealed with a weld. There are four large diffusion pumps which have a total pumping speed into the vacuum vessel of about 2000 liters per second for hydrogen. The pumps use Freon refrigerated baffles. The base pressure of the machine is about 3×10^{-8} Torr, mostly water vapor.

The systematic study of the influences of impurities in ATC has not started, but discharge cleaning of three to five thousand pulses of about 20 kA for about 2 msec at a pressure of about 1×10^{-5} hydrogen is sufficient to allow production of reproducible discharges (which will be discussed in Sec. IV). The pulse rate is 0.5 to 1 per second.

The Ohmic heating transformer and the vertical field coils were assembled after the vacuum vessel was installed in the toroidal field coils. The positions of these coils are shown to scale in Fig. 3 and the distribution of their turns is given in Table III. The field of the vertical field coils is nearly uniform, which means that the vertical stability is weak. This was a design compromise (which can probably be improved) chosen because it was considered important to connect the coils in series. A second factor was the desirability of having the Ohmic transformer coils and the vertical field coils inside composite coil holders (see Figs. 2 and 3).

The Ohmic heating transformer design provides a magnetic field less than 34 G in the pre-compression plasma volume at maximum OH bias current (10 kA). This coil system produces 0.24 V-sec with the design value of 10 kA in the Ohmic transformer coils.

The electrical circuit of the device is shown in Fig. 4 and a typical operating cycle is shown in Fig. 5. The Ohmic transformer is initially charged to some value (6 kA in Fig. 5) and at the initiation of the discharge the high voltage Ohmic heating capacitor bank is discharged to give a large initial voltage. When the voltage falls to that of the low voltage bank, it discharges and drives down the current in the Ohmic heating transformer at a slower rate, providing a voltage to maintain the pre-compression plasma. The equilibrium vertical field current is provided by a high power amplifier which can provide 2.4 kA. It is controlled by a function generator which is adjusted after successive discharges to achieve a satisfactory plasma.

The compression is carried out by pulsing a capacitor bank in parallel with the amplifier to increase the vertical field current. The rise time is about 2 msec. There is no provision, at present, to maintain the vertical field current after compression. The compression bank is crowbarred when the capacitor bank is discharged.

Preionization is provided by two turns inside the vacuum vessel which are connected to a 50 kW, 100 - 200 kHz oscillator which provides about 1 kV/turn. The preionization plasma has an electron density of $1 - 2 \times 10^{11}$ cm^{-3}.

Several papers which describe some of the design and engineering aspects of ATC have been published.[7]

IV. MHD BEHAVIOR OF PLASMA IN ATC

The initial operation of ATC has been concerned with producing a pre-compression plasma suitable for compression and then to compress it. The first phase of this program has been carried out and will be discussed here. We will consider the gross characteristics of the discharge, i.e., the current, density, and position and their behavior during compression. The documentation of the temperature is under active study, but is incomplete at this time and we will not discuss it except to note that the data indicate that the objective of producing a pre-compression discharge with T-3 parameters has been met.

Most of the usual diagnostic apparatus available on tokamaks is available on ATC and includes 2 mm and 4 mm microwave interferometers; a fast neutral detector; a ruby laser Thomson scattering system to determine the electron temperature and density; soft x-ray detectors to determine the electron temperature from bremsstrahlung; Rogovskii coils to determine the plasma current, vertical field current, and Ohmic heating transformer current; magnetic pickup loops to determine the plasma position; and voltage pickup loops.

The initial operation has been carried out at 14 kG toroidal field at 90 cm rather than 20 kG to decrease the risk of mechanical failure and also to increase the rate of taking data.

Figure 6 shows a sample of data obtained during a discharge which was compressed. Figure 7 shows the same data in graphical form. First note the similarity of the plasma current, vertical field current, and Ohmic transformer current to the pattern of Fig. 5. Note that the pre-compression plasma is established with a major radius of 90 cm and that the current and voltage traces are very similar to those obtained in ST and T-3 for similar currents. The proper voltage to incorporate into a conductivity calculation is, as always, somewhat uncertain, but if we use the value when the rate of change of current is small, we get about 20 μΩ for the discharge resistance which gives about 100 eV for the electron temperature, assuming a = 17 cm, uniform T_e, and Z = 1. Since resistivity is similar to that observed on ST and T-3 for much hotter discharges, and the x-ray bremsstrahlung and Thomson scattering measurements of T_e for this type discharge on ATC gives a much larger T_e, we assume that the effective Z is perhaps as large as 5 or 6 and that there are a large number of impurities in the discharge. The spectroscopic study of ATC has not started.

The vertical field required for equilibrium could be determined from Eq. (1) if the pressure and current distributions were known, which is not usually the case. Thus, the comparison of observed and theoretical values of the vertical field is not precise. A useful exercise is to calculate the quantity l_i,

$$l_i = \frac{cB_v R}{I_p} - \ln \frac{8R}{a} + \frac{3}{2} = \beta_p + \frac{\ell_i}{2} \quad . \qquad (6)$$

Even when no measurements of temperature or current distribution exist, knowledge of the value of l_i can give some insight into these quantities. For example, for uniform current density and $\beta_p = 1$

$\lambda_i \simeq 5/4$. Values of λ_i much larger than 5/4 would indicate either strong peaking of the current, or very high β_p, or both. In discharges otherwise thought to have low average temperatures a large λ_i tends to indicate the presence of runaway electrons which contribute to β_p. It should be noted that the increase in λ_i due to concentration of the discharge current to small minor radii is seldom sufficient to make $\lambda_i > 2$, and at such high values the likelihood of a low-m kink instability is high. The values of λ_i just before and just after compression for the discharge in Fig. 6 are 0.5 and 0.6, respectively. Thus, without any knowledge of the temperature or current distribution we can conclude that this discharge did not have a large number of runaway electrons or a strongly peaked current distribution.

The electron density is measured at three major radii, 90 cm, 65 cm, and 38 cm with 4 mm, 4 mm and 2 mm interferometers, respectively. The density at 65 cm is initially very low and then increases and decreases as the plasma column moves by during the compression. The density at the 38 cm radius is initially zero and then increases sharply as the compression takes place. In Fig. 6 the average density at 90 cm at the time of compression was 1×10^{13} cm. The maximum average density in the compressed plasma at 38 cm is 7×10^{13}. The density ratio is $\simeq 7$ which is in fair agreement with the value 5.6 given by the scaling laws.

The final check with the simple MHD theory is the value of the current in the compressed plasma. The scaling law gives a value of 2.37 for the ratio of the currents in the compressed and uncompressed plasmas. The value is 2.4 for the data in Fig. 6. It should be pointed out that the value of this ratio is dependent on the flux linking the plasma loop during the compression, and that, in order to observe the theoretical scaling the current in the Ohmic heating transformer coils must be carefully adjusted. It is true that the scaling laws of Table I apply to the plasma volume current, but the constraint on total flux conservation also applies. Therefore, while the total current adjusts to satisfy the flux conservation, some of this current flows as a skin current.

V. ACKNOWLEDGMENTS

The author acknowledges helpful discussions with Drs. R. Bol, H.P. Eubank, H.P. Furth, and W. Stodiek. He is also indebted to the operating crew of the ATC device for their help.

This work supported by U.S. Atomic Energy Commission Contract AT(11-1)-3073.

REFERENCES

[1] L. A. Artsimovich, Nuclear Fusion 12, 215 (1972).

[2] H. P. Furth and S. Yoshikawa, Phys. Fluids 13, 2593 (1970).

[3] V. S. Mukhovatov and V. D. Shafranov, Nuclear Fusion 11, 605 (1971).

[4] S. Yoshikawa, Phys. Fluids 7, 278 (1964).

[5] J. M. Greene, J. L. Johnson, and K. E. Weimer, Phys. Fluids 14, 671 (1971).

[6] V. D. Shafranov, Kurchatov Report IAE-1853 (May, 1969), Culham Translation CTO/661 (1969).

[7] Proceedings of the Fourth Symposium on Engineering Problems of Fusion Research, Washington, D. C., April 20-23, 1971 (IEEE, New York, 1971).

TABLE I

Scaling of Parameters with Slow Compression

	Constant-R a-Compression	R-Compression Type A	R-Compression Type B
Minor Radius a	c^{-1}	c^{-1}	$c^{-1/2}$
Major Radius R	Const.	c^{-1}	c^{-1}
Density n	c^2	c^3	c^2
Pressure P	$c^{10/3}$	c^5	$c^{10/3}$
Temperature T	$c^{4/3}$	c^2	$c^{4/3}$
Tor. Field at Fixed Point $B(R_o)$	c^2	c	Const.
Tor. Field at Plasma Axis B(R)	c^2	c^2	c
Plasma Current I	Const.	c	c
Plasma β_θ	$c^{4/3}$	c	$c^{1/3}$
Plasma β	$c^{-2/3}$	c	$c^{4/3}$
Plasma Potential ϕ	c^2	c^2	c
Vertical Field at Plasma Axis $B_z(R)$	$c^{7/3}$	c^3	$c^{11/6}$
Tot. Mag. Energy W_M	c^4	c^2	Const.
Tot. Plasma Energy W_p	$c^{4/3}$	c^2	$c^{4/3}$
Transform ι	Const.	Const.	Const.
Aspect Ratio R/a	c	Const.	$c^{-1/2}$

*Collisional time scale, so that $\gamma = 5/3$.

TABLE II

Toroidal Field Coils	
Coil i.d. (cm)	117
Coil o.d. (cm)	143.5
Major radius of coil center line (cm)	77
Field at coil center line (kG)	23.4
Coil current (kA)	37.5
Total NI (10^6 A turns)	9.0
Number of coils	24
Number turns/coil	10
Torus inductance (mH)	23.7
Torus resistance (mΩ)	8.8
Time constant (sec)	2.7
Equivalent square wave pulse (sec)	1.0
Resistive dissipation (MW)	27
Energy storage (MJ)	16.7
Power supply -	4 large generators arranged in 2 parallel pairs
Total weight of copper (lbs)	21,000
Centering force per coil (lbs)	380,000

TABLE III

	Inner (1)	Middle (2)	Outer (3)
Ohmic Heating Coils			
Major radius (cm)	52.0	93.0	122.0
Distance from midplane (cm)	23.0	36.8	19.1
NI (kA turns)	130	20	10
No. turns	13	2	1
Current (kA) max.	10	10	10
Self-inductance (set)		0.9 mH	
Resistive power dissipation (6 coils)		2.4 MW	
Energy storage (6 coils)		50 kJ	
Power supply		one large generator	
Shaping and Compression Coils			
Major radius (cm)	50.0	90.0	125.0
Distance from midplane (cm)	25.0	38.0	18.0
NI (kA turns) before compression	2.0	10.0	18.0
NI (kA turns) at max. compression	10.0	50.0	90.0
No. turns	1.0	5.0	9.0
Current (kA) max.	10.0	10.0	10.0
Self-inductance		2.06 mH	
Resistive power dissipation (6 coils)		700 kW	
Energy storage (6 coils)		250 kJ	
Power supply		High current amplifier plus capacitor bank	

FIGURE CAPTIONS

Fig. 1. Comparison of the type-A and type-B compression processes, showing initial and final configurations.

Fig. 2. Cutaway view of the ATC showing all major components except the structure, busbars, and plumbing.

Fig. 3. Schematic cross section of the ATC. Specifications for the toroidal field coils and the Ohmic heating and shaping coil sets 1, 2, and 3 are given in Table III. Initial and final plasma configurations are shown.

Fig. 4. Schematic electrical circuits of the Ohmic heating and shaping field coils.

Fig. 5. Typical ATC operating cycle. A generator-driven, quasi-dc primary current in the Ohmic heating coils is programmed down, thus inducing the plasma current, while a current in the shaping coils maintains correct equilibrium. After initial heating period, the shaping coil current is raised rapidly to effect plasma compression, thus multiplying plasma current.

Fig. 6. Data obtained for a compressed discharge in deuterium at 1×10^{-5} torr. Of these data the interpretation is self evident for the ohmic heating transformer current - OH; vertical field current - SF; plasma current - Ip; plasma loop voltage - V_l, and the electron density at 90 cm - n_e (note the different sweep duration). The trace of electron density at 38 cm - n_e is triggered 1 m sec before the compression. The traces marked B_θ are signals from local magnetic probes which are located at the positions shown on the diagram both above and below the vacuum vessel. The array of B_θ probes is used to sense the major radius of the plasma. At B_{θ_1}, and B_{θ_1} both the sum and difference signal are shown. The major radius is determined from analysis of the sum signals and the vertical shift from the difference. For example, from B_{θ_5} we observed that the plasma is shifted slightly up from the difference signal (the smaller signal). The trace showing B_{θ_1} and B_{θ_2} was triggered 1 m sec before the compression and shows a ratio of $B_{\theta_1}/B_{\theta_2}$ which indicates that the plasma major radius is about 38 cm. The difference signal at B_{θ_1}, shows a small downward shift for the compressed plasma. The signals marked c and d are the fluxes from toroidal loops located above and below the vacuum vessel at about the positions marked 1,2,3 on the diagram. c represents the sum of the fluxes through these loops and a represents the fluxes between loops 1 and 2. These data can be analyzed to give the major radius near 90 cm.

The traces marked a and b are currents in each of two pair of passive shorted copper rings connected to provide some vertical stabilization, but not to interfere with the motion along the major radius.. Trace a represents the current in coils at approximately the position marked 1 on the diagram and trace b is from a set of coils near position 2. These currents are sensitive indicators of the vertical motion of the plasma column and give results in agreement with the B_θ probes.

Fig. 7. The data of Fig. 6, replotted on a common time base.

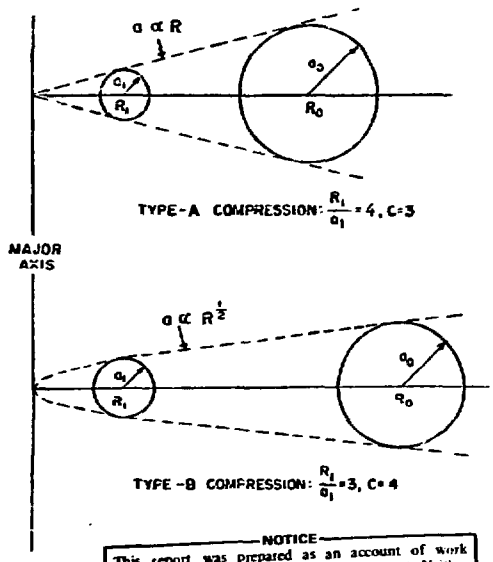

NOTICE
This report was prepared as an account of work sponsored by the United States Government. Neither the United States nor the United States Energy Research and Development Administration, nor any of their employees, nor any of their contractors, subcontractors, or their employees, makes any warranty, express or implied, or assumes any legal liability or responsibility for the accuracy, completeness or usefulness of any information, apparatus, product or process disclosed, or represents that its use would not infringe privately owned rights.

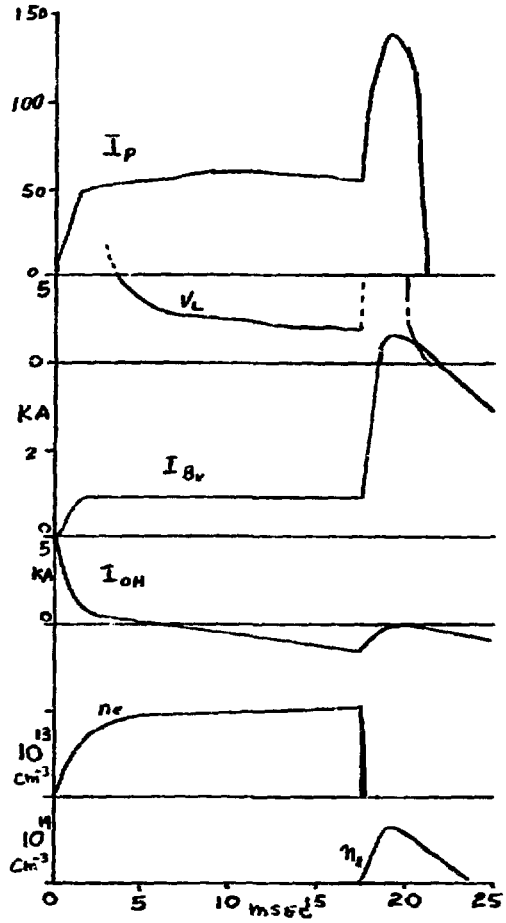

FIG. 7

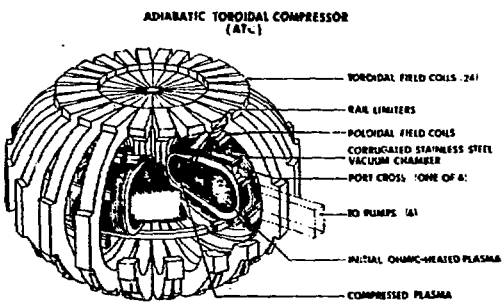

FIG. 2

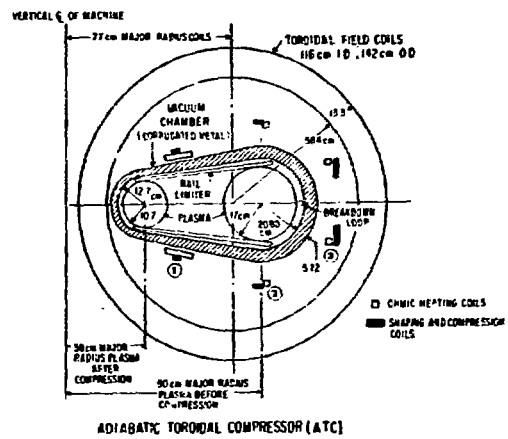

FIG. 3

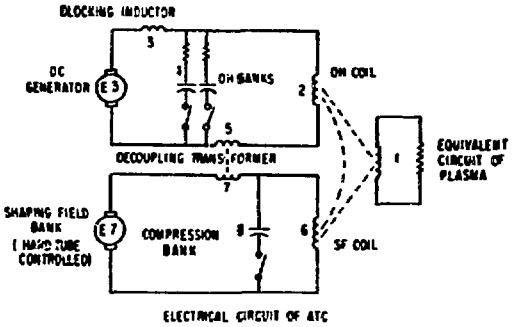

FIG. 4

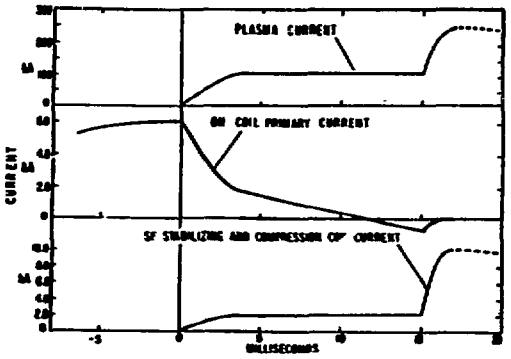

FIG. 5

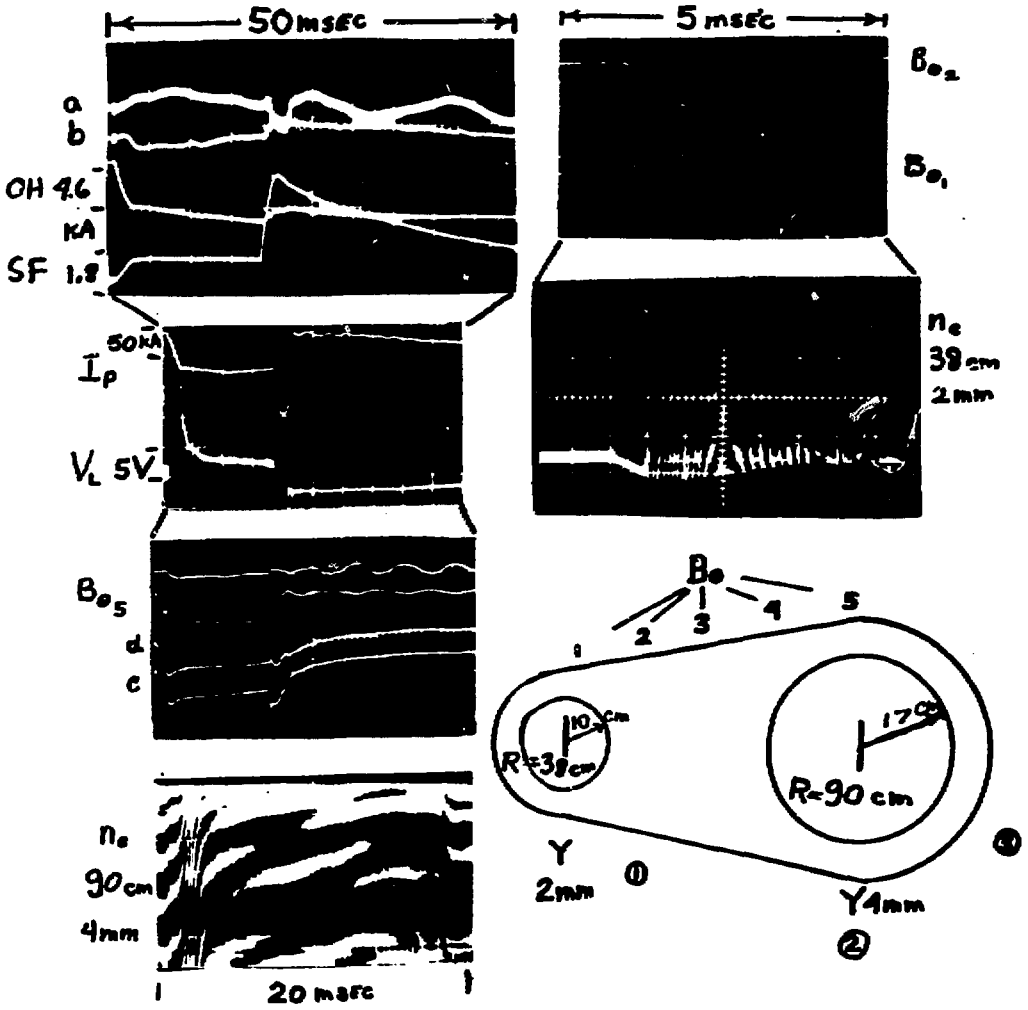

FIG. 6